Hopf Bifurcation in a Broken-Parity Pattern

L. Gil,[2] G. Balzer,[1] P. Coullet,[2] M. Dubois,[1] and P. Berge[1]

[1]*Service de Physique du Solide et de Résonance Magnétique–Commissariat à l'Energie Atomique, Ormes des merisiers, 91191 Gif-sur-Yvette CEDEX, France*

[2]*Institut du Non Linéaire de Nice, Université de Nice Sophia Antipolis, Parc Valrose, 06034 Nice CEDEX, France*

(Received 10 December 1990)

In this paper we report both experimental and theoretical results on a Rayleigh-Bénard convection experiment with a static spatially periodic forcing. For reduced Rayleigh number of order 100, the system undergoes a secondary Hopf bifurcation involving novel and surprising spatially inhomogeneous temporally periodic states. We give a description of these various inhomogeneous states, and develop a simple phenomenological model based on symmetry considerations which seems to capture all the essential qualitative features.

PACS numbers: 47.10.+g, 05.45.+b, 47.20.Ky

We have modified a standard large-aspect ratio, one-dimensional Rayleigh-Bénard experiment by adding regular arrays of small bumps on both the upper and lower plates of the convective cell.[1] The distance between two bumps has been chosen equal to the mean wavelength chosen by the free normal convection in the same experimental conditions, and the size of the knobs is about one-sixth of the height of the box. *A priori*, as we expected the hot fluid currents to rise vertically from the bottom bumps, the aim of this spatial forcing was to lock the roll positions and therefore to avoid the coexistence of various stable wavelengths at high Rayleigh number. But, in fact, it turns out that above the convection threshold, the spatial forcing gives rise to an unexpected parity-symmetry-breaking steady state.[2,3] The currents are no longer vertical, but tilted either to the left or to the right, making an angle θ with the vertical line. As for the ferromagnetic transition, this symmetry breaking can lead to topological parity defects asymptotically connecting regions with opposite incline. When further increasing the Rayleigh number, the system reaches time-dependent regimes, characterized by an oscillating of the direction of the hot fluid current around the mean tilted position. Surprisingly these first time-dependent states are really not homogeneous. In this Letter we report some typical situations with coexistence of stationary and oscillating regions, which cannot be explained by means of a subcritical bifurcation. We develop a phenomenological model based on Ginzburg-Landau-type equations[4] and describe the mechanisms responsible for this unexpected spatial behavior.

Recent one-dimensional experiments on Rayleigh-Bénard convection[5,6] have already reported the existence of a secondary Hopf bifurcation occurring on a stationary space-periodic pattern. From a theoretical point of view, a quantitatively good agreement has been obtained with phenomenological models which consider only two order parameters, one for each symmetry-breaking transition.[7] In all cases, even for a subcritical secondary Hopf bifurcation, the amplitude of the oscillations near the threshold has always been reported to be almost the same throughout the cell. On the contrary, for the forced Rayleigh-Bénard convection, the first time-dependent states are really not homogeneous. Besides the situations where the inhomogeneities are obviously related to the presence of parity defects, there exist some unexpected cases where the hot currents, for example, all tilted to the right, are stationary in the left part of the convection cell and oscillating in the right part (Fig. 1). Changing the Rayleigh number varies the amplitude of

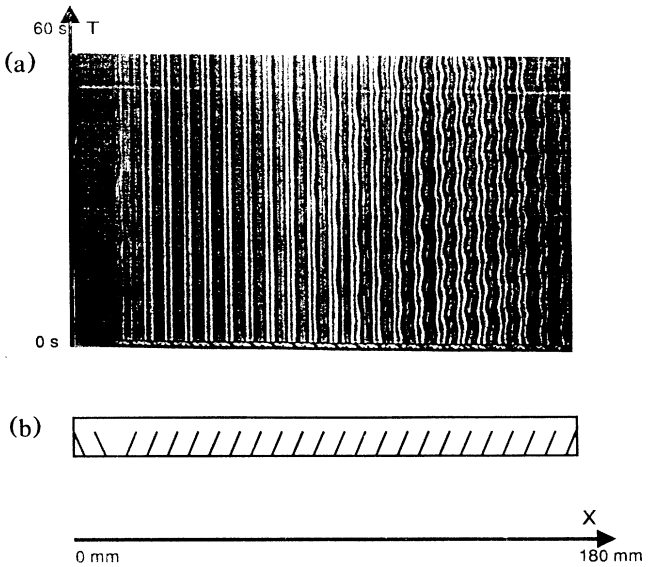

FIG. 1. Experimental results obtained for $\epsilon=150$. (a) Black corresponds to the hot fluid currents and white to the cold ones. The picture shows the evolution of the convective pattern vs x and t. (b) Schematic plot illustrating the mean tilting of the hot current.

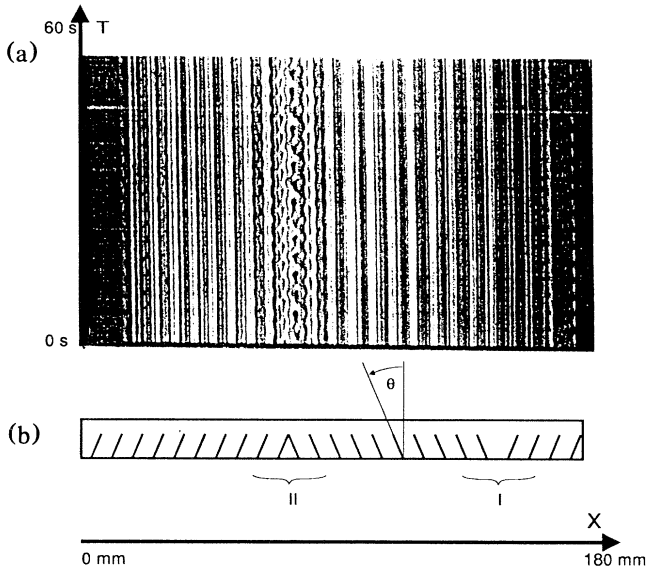

FIG. 2. Same as for Fig. 1 but now $\epsilon=80$ and the spatial structure displays a parity defect of type II almost in the center of the box.

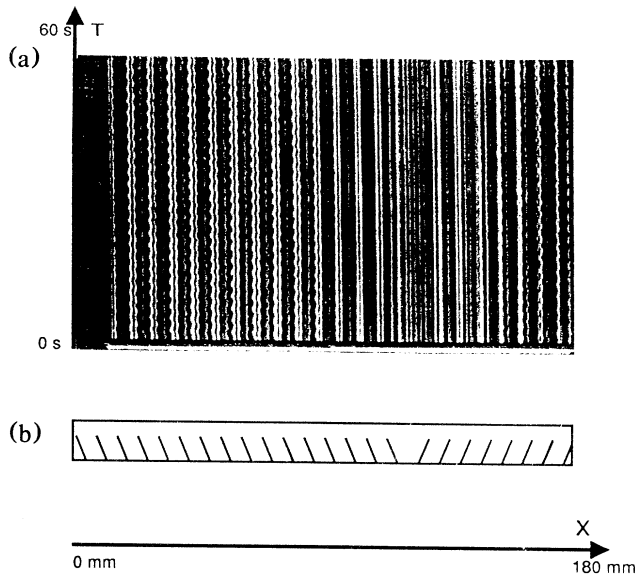

FIG. 3. Same as for Fig. 1 but now $\epsilon=100$ and the spatial structure displays a parity defect of type I almost in the center of the box.

the oscillations as well as the length of the stationary region. This situation is absolutely symmetric and an incline of the hot currents to the left corresponds, for the same value of the temperature gradient, to a state with a left-oscillating and a right-stationary region.

The situation is much more complex when topological parity defects are present, especially because the two kinds of defects do not play a symmetric role. The defects of type I, connecting a region with positive θ at $-\infty$ to one with negative θ at $+\infty$, are usually associated with a decreasing or even a vanishing of the oscillation amplitude at the defect core [Fig. 2(b)]. On the contrary, at the core of type-II defects [$\theta(-\infty)<0$, $\theta(+\infty)>0$] higher amplitudes are often observed. We want to report here two typical situations. In the first one obtained at $\epsilon=(\mathrm{Ra}-\mathrm{Ra}_c)/\mathrm{Ra}_c=80$, all of the tilted pattern is stationary except the core of a defect (II) which slowly oscillates (Fig. 2). On the contrary, in the second situation, $\epsilon=100$, only the core of the defect (I) is stationary (Fig. 3). Not only can the amplitude and the frequency change, but also the defect shapes may change. For example, we have observed type-II defects separating regions with stationary tilting from regions with oscillating hot currents (Fig. 4).

From a phenomenological point of view, the description of both the parity transition and the breaking of the time translational symmetry requires two order parameters A and B slowly varying with respect to space and time. The angle θ, which is one of the most relevant macroscopic physical quantities, should then be expressed versus A and B as

$$\theta(x,t)=A(x,t)+\mathrm{Re}[B(x,t)e^{i\omega t}]\xi(x)+\cdots, \quad (1)$$

where ω is the pulsation and $\xi(x)$ the spatial mode of the Hopf bifurcation, and where the dots stand for higher-orders terms. A and B may be considered as measures of the amount of symmetry breaking since $A=0$ corresponds to the parity-symmetric situation and $B=0$ to the absence of oscillation. In spite of the spatial inhomogeneity of the temporal behavior, we choose $\xi(x)$ to be constant in the box, as is usual for a Hopf bifurca-

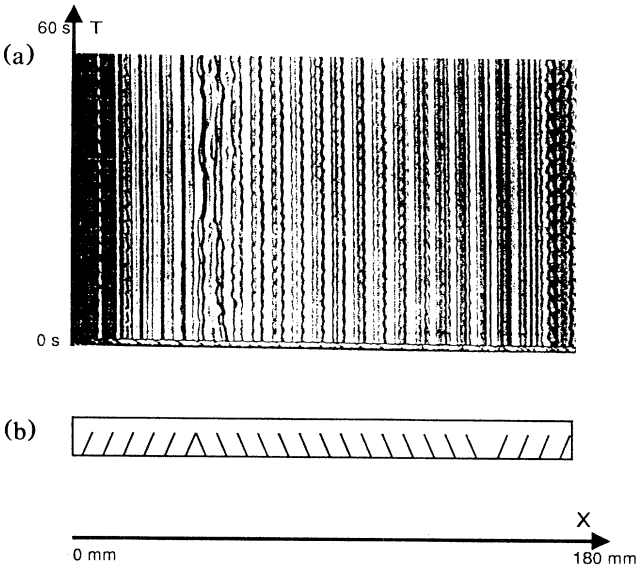

FIG. 4. Same as for Fig. 1 but now $\epsilon=100$. The parity defect of type II near the left boundary separates a stationary region from an oscillating one.

tion in a closed system. The time evolution equations for A and B can then be derived from symmetry considerations. The global invariance of the set of solutions with respect to the parity ($x \to -x$, $\theta \to -\theta$) and the time translation ($t \to t+t_0$) implies that the equations are invariant under the following transformations:

$$x \to -x, \quad A \to -A, \quad B \to -B,$$
$$t \to t+\phi/\omega, \quad A \to A, \quad B \to Be^{i\phi}. \tag{2}$$

Experimentally the characteristic variation lengths of A and B are almost the same. Assuming then the two order parameters to be of the same order of magnitude leads to equations of the form

$$\frac{\partial A}{\partial t} = i\delta\left(B\frac{\partial \bar{B}}{\partial x} - \bar{B}\frac{\partial B}{\partial x}\right) + (\mu + \nu|B|^2)A + \beta A^3 + \alpha\frac{\partial^2 A}{\partial x^2} + O(4),$$
$$\frac{\partial B}{\partial t} - z_4 A\frac{\partial B}{\partial x} = \left(z_{11} + z_{12}A2 + z_{13}\frac{\partial A}{\partial x}\right)B + z_2|B|^2 B + z_3\frac{\partial^2 B}{\partial x^2} + O(4), \tag{3}$$

where δ, μ, ν, β, and α are real coefficients while the z_i are complex. In the regime of parameters of our interest ($\epsilon \simeq 70$), i.e., quite close to the second bifurcation, the parity-breaking structure is experimentally very stable, and seems never to be affected by the dynamical behavior. In what follows, we will then assume that δ and ν are equal to zero such that the equation for A exactly reduces to the Landau equation for the ferromagnetic transition.

On the contrary, the coupling terms in the second equation cannot be neglected, if one wants to understand the spatial inhomogeneity. At the lowest order, $z_4 A \times \partial B/\partial x$ is the first term invariant under the transformations (2). Its real part acts as an effective group velocity and we will show later that it is relevant for the distinction between the absolute and convective instability mechanisms.[8] Its imaginary part has to deal with the preferred wave vector of the oscillation and the Eckhaus instability.[9] The other coupling terms renormalize in a way, an already existing coefficient. In the effective B eigenvalue the real parts of $z_{12}A^2$ or $z_{13}\partial A/\partial x$ describe modifications of the oscillation amplitude due to the parity pattern. When topological parity defects are present, the first term corresponds to localized symmetric variations, while the effect of the other depends on the defect sign. The imaginary parts of these coefficients stand for local renormalizations of the oscillation frequency, with a symmetric and an antisymmetric action, respectively.

We have numerically simulated Eqs. (3) with a second-order accurate space and time finite-difference scheme. We have imposed rigid boundary conditions for both order parameters [$A(0,t)=B(0,t)=0$, $A(L,t)=B(L,t)=0$] and have used numerical boxes of various lengths from 60 to 300, with a number of collocation points from 300 to 8192. Finally, a very small permanent Gaussian noise has been added in order to simulate the experimental fluctuations and to sustain structures.[10,11] For the sake of simplicity, we have chosen the control parameters such that each numerical simulation brings to the fore only one single mechanism. However, the results are quite generic and would persist for a wide range of parameters.

Figure 5 (part 1) illustrates the role of the $z_4 A\,\partial B/\partial x$ coefficient, and is related to the experimental Fig. 1. All the coupling terms have been taken equal to zero, except the real part of z_4 [$\mathrm{Re}(z_4) < 0$]. The effective group velocity is homogeneously positive. Therefore, near the left boundary, every small perturbation around $B(x=0,t)=0$ simultaneously grows and moves to the right of the box. In the absolute instability case, the growth rate is more important than the group velocity and the oscillation takes place near the left boundary. In the opposite case, we are dealing with a convective instability and the amplitude of the oscillation, almost zero in the neighborhood of the left boundary, reaches a significant nonzero value only at a certain distance from the boundary. Note that for this mechanism which does not depend on the presence of defects, the role played by the lateral walls is crucial since without any rigid boundary condition, B would never have reached a constant zero value.

For the simulation of Fig. 5 (part 2), we have used exactly the same parameter values as before but the initial field A has been chosen in order to display two topological parity defects of opposite sign. Now the effective group velocity is positive near the left and right boundaries, but negative between the two defects. Therefore, in a convective unstable regime, every small growing perturbation moves to the left until it reaches the negative-group-velocity region and then stops. This mechanism explains why a type-II defect close to a boundary may separate stationary and oscillating regions.

The numerical results of Figs. 5 (parts 3 and 4) illustrate the role played by the asymmetric renormalization of the oscillation eigenvalue and are related to the two experimental cases shown in Figs. 2 and 3. All the coupling coefficients have been taken equal to zero except the real part of z_{13} which was chosen strictly negative. In the first case, the B eigenvalue [$\mathrm{Re}(z_{11})$] is weakly negative in order to remove all oscillations when coupling terms are not present. At the defect-II core, the parity gradient is negative and therefore $z_{13}\partial A/\partial x$ is a positive renormalization of the growth rate. For the second case, $\mathrm{Re}(z_{11}) > 0$, but at the core of a type-I defect, the parity gradient sufficiently decreases the effective eigenvalue to locally stop the oscillation.

In conclusion, the simple theoretical model we have developed is in quite good qualitative agreement with the experimental data. Based on symmetry considerations,

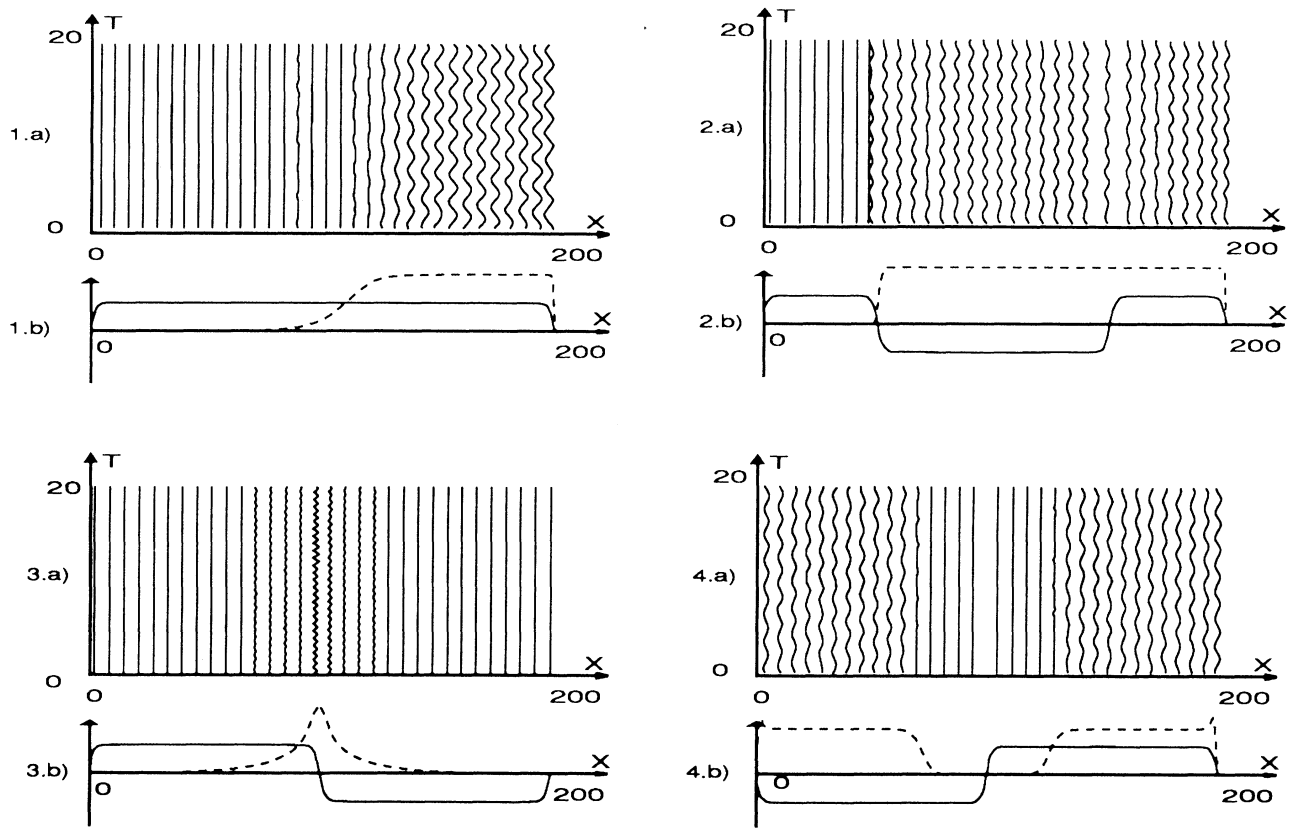

FIG. 5. Numerical simulation of Eq. (3) with $\mu=\alpha=\beta=1$, $\delta=\nu=0$, and $z_2=-1+0.7i$, $z_3=1+0.3i$, $z_{12}=0$. The noise amplitude is 10^{-8}. (a) The evolution of the positions of the hot fluid current vs x and t. (b) A (solid line) and $|B|$ (dashed line) vs x. (1) $z_{11}=1$, $z_4=-6$, and $z_{13}=0$. (2) $z_{11}=1$, $z_4=-6$, and $z_{13}=0$. The only difference from (1) is the presence of topological parity defects of types I and II. (3) $z_{11}=-0.1$, $z_4=2$, and $z_{13}=-2$. (4) $z_{11}=1.1$, $z_4=-2.1$, and $z_{13}=-3$.

the results are quite generic and should have to apply to all secondary oscillatory instabilities of a closed system which has already broken the parity symmetry. They also shed new light on the distinction between open and closed systems.

We acknowledge the INRIA Sophia-Antipolis where the numerical simulations presented in this paper have been performed, DRET (Contract No. 88CO145) (Direction des Recherches Etudes et Techniques) for financial support, and the European Economic Community for the contract entitled "Spatio-Temporal Chaos in Extended System." Institut du Non Linéaire de Nice is UMR CNRS No. 129.

[1]The convection cell is rectangular, with a depth d of 9 mm and horizontal aspect ratios respectively equal to 0.28 and 20. The distance between two bumps on the same plate is $0.42\lambda_c$ with $\lambda_c=2d$, which leads to 48 convective rolls. The upper and lower arrays of bumps are shifted one from the other and are made of the same material as the plates.

[2]P. Bergé, Model. Math. Anal. Num. **23**, 371 (1989).

[3]G. Balzer, P. Coullet, Y. Pomeau, P. Berge, M. Dubois, and L. Gil, C. R. Acad. Sci. Paris Ser. 2 **312**, 585 (1991).

[4]For a general discussion of Ginzburg-Landau-type equations see, for example, J. T. Stuart, J. Fluid Mech. **9**, 353 (1960), and K. Stewartson and J. T. Stuart, J. Fluid Mech. **48**, 529 (1971), for the theoretical part, and M. Provansal, C. Mathis, and L. Boyer, J. Fluid Mech. **182**, 1 (1987), and S. Douady, thesis, University Paris VI, 1989 (unpublished), for the experimental results.

[5]M. Dubois, R. Da Silva, F. Daviaud, P. Berge, and A. Petrov, Europhys. Lett. **8**, 135 (1989).

[6]S. Ciliberto and P. Bigazzi, Phys. Rev. Lett. **60**, 286 (1988).

[7]P. Coullet and G. Iooss, Phys. Rev. Lett. **64**, 866 (1990).

[8]J. M. Chomaz, P. Huerre, and L. G. Redekopp, Phys. Rev. Lett. **60**, 25 (1988).

[9]V. Eckhaus, *Studies in Nonlinear Stability Theory* (Springer-Verlag, Berlin, 1965).

[10]R. Deissler, J. Stat. Phys. **40**, 371 (1985).

[11]P. Coullet and F. Plaza, University of Nice report, 1990 (to be published).